Journal of Power Sources 268 (2014) 1–6

Contents lists available at ScienceDirect

Journal of Power Sources

journal homepage: www.elsevier.com/locate/jpowsour

Scattering resonance enhanced dye absorption of dye sensitized solar cells at optimized hollow structure size

Min-Chiao Tsai [a], Jeng-Yi Lee [b], Ya-Chen Chang [a], Min-Han Yang [a], Tin-Tin Chen [a], I-Chun Chang [a], Pei-Chi Lee [d], Hsin-Tien Chiu [c], Ray-Kuang Lee [b], Chi-Young Lee [a, *]

[a] Department of Materials Science and Engineering, National Tsing Hua University, Hsinchu, Taiwan
[b] Institute of Photonics Technologies, National Tsing Hua University, Hsinchu, Taiwan
[c] Department of Applied Chemistry, National Chiao Tung University, Hsinchu, Taiwan
[d] Department of Applied Cosmetology, Master Program of Cosmetic Science, Hungkuang University, Taichung, Taiwan

HIGHLIGHTS

- Hollow spheres with size matching the dye's absorption band can greatly enhance light harvesting.
- The hollow spheres of 450–550 nm harvest light most efficiently for N719 dye molecules.
- Hollow spheres have higher conversion efficiency per unit volume than that of mesoporous spheres.

ARTICLE INFO

Article history:
Received 11 March 2014
Received in revised form
20 May 2014
Accepted 3 June 2014
Available online 12 June 2014

Keywords:
Mie scattering
Mie theory
Simulation
Resonance
Nanoparticle

ABSTRACT

This study elucidates the size effect on dye-sensitized solar cells (DSSCs) by synthesizing highly uniform hierarchical hollow sphere TiO_2 samples, with the diameters from 220 nm to 800 nm. Experimental results indicate that the optimum conversion efficiency using N719 dye can be achieved around 5.5%, as the diameter of hierarchical hollow spheres is 450–550 nm. According to the incident photon-to-current conversion efficiency (IPCE) spectra, large-sized hierarchical hollow spheres significantly enhance the light harvesting by scattering; whereas small-sized hallow spheres (<360 nm) improve negligibly. Additionally, mesoporous and solid spheres with an identical diameter, 440 nm in this study, are also studied as a comparison. Our results demonstrate that hollow spheres perform the same conversion efficiency as that of mesoporous spheres owing to the equivalent adsorption of dye molecules in both hierarchical structures – regardless of the surface area of the interior of mesoporous structure, which shows that hollow spheres have higher conversion efficiency per unit volume than that of mesoporous spheres.

1. Introduction

Hierarchical structured materials, in which primary units are stacked from nano- to micron- scale by a sequence with different morphologies, have attracted considerable interest in recent years, owing to their fascinating properties [1–5]. Such materials possess properties from their bulk-like micro structures, while still maintain a high surface area as the primary nanostructure. Interesting properties in different hierarchical structures include a fast electrolyte diffusion, effective charge transportation, and improved light scattering [3,6–9]. Moreover, promising properties are continually discovered, in which efficient charge separation is observed in an urchin-like structure composed of consecutive grains with a gradually increasing size from the tip to the center of the structure, resulting in being capable of leading electrons and holes to flow to opposite direction. Those charges have been created, owing to variation of the surface potential of different-sized grains [10].

Based on the above discoveries, researchers have introduced various hierarchical structure materials in various fields such as photocatalysts [7,10,11]. Li ion battery [12–14], dye-sensitized solar cells [15–20], and evolution of H_2 [21]. Among these hierarchical structures, spherical hierarchical particles (including mesoporous and hollow spheres) have emerged as a prominent area of study to achieve efficient light harvesting by the light scattering effect in a micron structure [22–27]. Cao and coworkers first described the

* Corresponding author. Tel.: +886 3 5717131x35335.
E-mail address: cylee@mx.nthu.edu.tw (C.-Y. Lee).

http://dx.doi.org/10.1016/j.jpowsour.2014.06.015
0378-7753/

feasibility of using spherical mesoporous ZnO particles as electrodes for DSSC applications. The authors also demonstrated that mesoporous spheres can harvest more incident light by a higher dye loading and scattering [20,21]. In the subsequent studies, TiO_2 mesoporous spheres were synthesized to replace ZnO as electrodes with an excellent performance, in which the efficiency could reach 10% [9,28]. As the particle size approaches the wavelength of incident light, on which the resonance effect light-scattering emerges, which is known as Mie's scattering effect [29]. Resonant peaks appear in the scattering (extinction) spectrum only for some specific sizes. To obtain this optimum size, size-dependent investigations of hierarchical mesoporous spheres were conducted to determine its influences on the performance of DSSC. The highest conversion efficiency was observed for the mesoporous spheres of 450–590 nm in size [30,31]. However, hierarchical hollow spheres were also used as DSSC electrodes for the same purpose. Additionally, the shells of a hollow structure trap the light in the interior of structure by reflections and diffractions, subsequently allowing the dye molecules on the shell a greater opportunity to absorb light source and increasing the efficiency significantly. Instead of using geometrical optics to the illustration, which is appropriate only for an object that is significantly larger than incident light, Tsai and coworkers theoretically demonstrated that a hollow sphere has the same absorption power as that of a solid sphere when the shell thickness is thick enough by extending Mie's scattering theory [7]. This theoretical background leads us to the motivation on using hollow spherical structures for light harvesting. To the best of our knowledge, investigations on these two promising structures as well as the feasibility of using different sized hollow spheres in DSSC applications still lack. Here, highly uniform sized hollow spheres are synthesized by a self-templating method for DSSC applications. A comparison between mesoporous and solid spheres with the same diameter is also performed.

2. Experiments

2.1. Synthesis of hollow spheres

Details of the method used in this study with some modifications to prepare amorphous precursor spheres can be found in our earlier work [32,33]. Briefly, nanoparticles of various sizes were synthesized by using titanium isopropoxide (TTIP, 97%, Aldrich), and octanoic (99.5%) acid in anhydride alcohol (99.5%). All chemicals were purchased from the Aldrich Company and used directly without pretreatment. Octanoic acid was injected into 375 mL ethanol, followed by the addition of 3 mL (10 mmol) of TTIP. A solution with a variable amount of deionized water and ethanol with equal ratio was subsequently added and kept stationary for 2 h to induce hydrolysis and condensation. The precipitate was then collected by centrifuging and washed by ethanol for several times. After washing, the residual ethanol was removed by placing it in an oven at 100 °C for overnight. By a typical hydrothermal process, particles in the shape of hollow-spheres were prepared as follows: 0.2 g of precursor spheres was dispersed in 25 mL NaF solution with a concentration of 0.05 M. The mixture was then sealed in a 45 mL Teflon-lined stainless autoclave, followed by heat treatment at 190 °C for 18 h. Finally, the hollow spheres were washed with water several times and dried in an oven at 100 °C overnight.

2.2. Preparation of DSSCs

DSSCs were fabricated as follows. A TiO_2 photoelectrode was prepared on F-doped tin oxide (FTO) substrates by doctor-blading, with a paste containing 0.2 g of TiO_2 powder and 0.02 g of polyethylene glycol (PEG, Mw = 35,000) in 300 μL of 5% acetic acid, 20 μL of deionized water and 30 μL of acetylacetone, followed by sintering at 450 °C for 30 min. The TiO_2 photoelectrodes have an average thickness of 7–9 μm, measured by an Alpha-step (Veeco, Detak150). In this study, the various TiO_2 photoelectrodes are denoted as HS, SS and MS for hierarchical hollow spheres, solid sphere and mesoporous spheres, respectively. The TiO_2 photoelectrodes were then coated with commercial N719 dye by immersing TiO_2 photoelectrode in 0.3 mM N719 solution at room temperature overnight. Next, the Pt electrode was prepared by spin-coating the H_2PtCl_6 solution on the FTO glass, followed by sintering at 350 °C for 30 min. Finally, DSSC was assembled as a sandwich type, and a spacer (SX1170-60) was applied. A commercial redox electrolyte (Electrolyte_E-1_MPN-based, Tripod) containing I^-/I^{3-} was used. The *J–V* curves were recorded by using a Keithley 2400 instrument under AM 1.5 (Newport). Moreover, dye desorption was performed by immersing a dye-absorbed electrode in 50 mM NaOH solution for 1 h. The resulting solution corresponding to the dye loading was analyzed by the UV–visible system (Avantes UV spectrum).

3. Results and discussion

Various-sized mono-dispersed TiO_2 anatase hollow-spheres are synthesized by using amorphous TiO_2 spheres as both the precursor and template via a self-templating method. Fig. 1 shows the scanning electron microscopy (SEM) image of hierarchical hollow spheres with a mean diameter ranging from 220 nm to 810 nm. Based on this method, highly uniform hollow spheres with a standard deviation of approximately 5% in diameter are calculated from 200 spheres of each sample from SEM images. The nanoparticles are also prepared for comparison by crushing hollow spheres. As shown in Fig. 1a, the morphology of hollow spheres are destroyed completely by smashing hollow spheres in an agate mortar. Additionally, the crystalline structure of various sized hollow spheres is characterized by X-ray diffraction pattern (XRD) (Fig. S1). Analysis results indicate that all different sized amorphous solids are converted into to anatase hollow spheres during the reaction. An attempt is also made to more thoroughly understand the constitution of highly uniform hollow spheres by using transmission electron microscope (TEM) to examine the hierarchical structure of hollow spheres with different sizes (Fig. 2). This figure clearly reveals the empty interior of spheres by the contrast of hollow spheres (Fig. 2a–c) and the shells containing nano primary particles of 10–30 nm in size (Fig. 2d–f), strongly implying a hierarchical structure of all hollow spheres. Notably, the primary particles have a unique rhomboid shape enclosed by (101) and (001) active faces with a high photocatalytic ability for hierarchical hollow spheres [7,11]. Moreover, the shell thickness of hierarchical hollow spheres has a similar thickness of around 50 nm, regardless of its size. The primary particle size of various hollow spheres is also thoroughly evaluated by estimating the average particle size of shells by Scherrer equation based on plane (101). Table 1 summarizes those results. This table reveals that the average primary particle size of the hierarchical hollow sphere decreases slightly from 14.6 nm to 12.6 nm as the diameter of template solid spheres increase from 220 nm to 800 nm. This finding closely corresponds to the surface area measurements taken by Brunauer–Emmett–Teller measurement (BET), 47.5 $m^2\ g^{-1}$ for the smallest hollow sphere and rises to 56 $m^2\ g^{-1}$ with an increasing sphere size. Moreover, two groups of pore-size distribution of 8 nm and 35 nm shown in BJH measurement indicate that the hollow spheres with a shell mixed with two kinds of pores can have a unique hierarchical structure which was featured by bimodal pores distributions existing in materials [34,35].

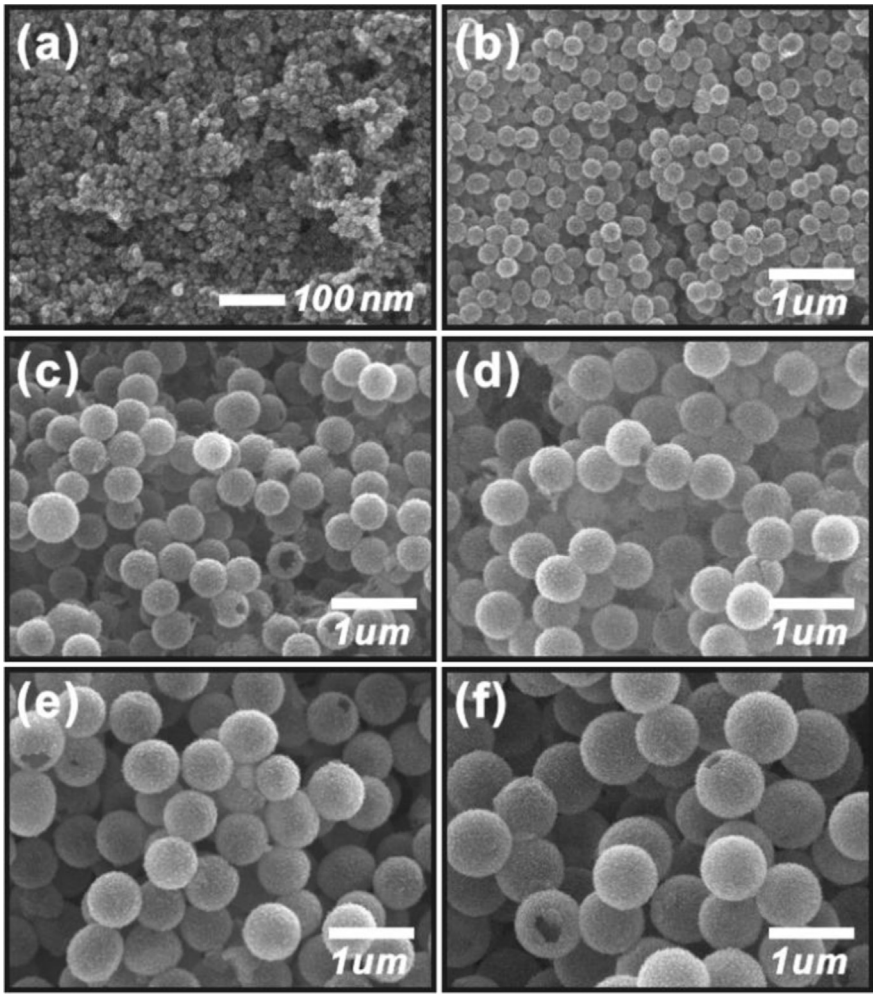

Fig. 1. SEM images of hierarchical structured hollow spheres with various sizes for the electrodes of a dye-sensitized solar cell. (a) Nanoparticles with 30 nm from crushed spheres. (b) Hollow spheres of 220 nm. (c) 440 nm. (d) 540 nm. (e) 630 nm. (f) 810 nm.

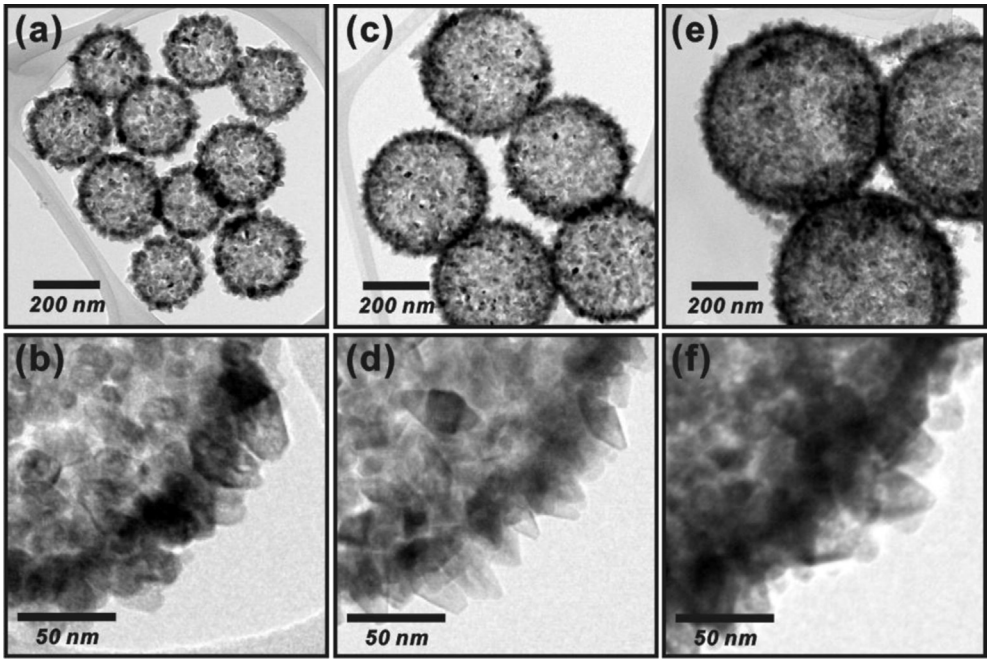

Fig. 2. TEM images of hierarchical structured hollow spheres with various sizes for the electrodes of dye-sensitized solar cell. (a, b) Hollow spheres of 220 nm. (c, d) 440 nm. (e,f) 630 nm.

Table 1
The summary of surface area and crystalline size.

Sample (nm)	220	440	620	800
Grain size (nm)	14.6	13.2	13.1	12.6
Surface area ($m^2\ g^{-1}$)	47.5	52.1	55.9	54.0
Pore sizes (nm)	31.9	22.5	17.4	18.5

This study also investigates how size affects hollow spheres as DSSC photoelectrodes. Photoelectrodes of various sized hollow spheres are prepared by loading the TiO_2 sphere on FTO substrates with a layer thickness ranging from 7 to 9 μm. The photocurrent–photovoltage (I–V) curves of DSSC electrodes made by various sized hollow spheres are then examined under an AM 1.5 light source (Fig. 3). Table 2 summarizes the corresponding photovoltaic characteristic parameters. This table also includes the photoelectrode made by nanoparticles from smashed hollow spheres for comparison. According to this table, the largest open circuit voltage (V_{oc}), 0.795 and 0.783 V, occurs for the electrodes HS220 and NP, respectively, and around 0.76 V for the photoelectrodes made by hollow sphere with 300–800 nm diameter, showing no obvious correlation between V_{oc} and the diameter of hollow spheres. Of these electrodes, the highest short-circuit photocurrent density (J_{sc}) around 12 mA cm^{-2} appears in HS550 and HS440, resulting in the highest conversion efficiency (η) of 5.6 for both HS550 and HS440, whereas the lowest η of 3.9 is observed in the cell of HS220. As is well known, the dye adsorption capacities of electrodes significantly affect the DSSC performance. Closely examining the dye adsorption reveals that dye adsorption increases with an increasing diameter of hollow spheres, which correlates well with the surface area measurements and primary particle size calculations in Table 1. A high J_{sc} is normally attributed mainly to high dye adsorption. However, in this study, the highest J_{sc} is (NOTE: Consistent verb tense) obtained for HS440 and HS550; whereas, HS880 and NP does not, which has the highest dye loading around 11.6 nM cm^{-2} mm^{-1} among all samples.

Above observations suggest that scattering greatly facilitates the generation of a photocurrent by enhancing the light harvest capability of dye molecules on spherical hollow spheres with an appropriate size. Next, the extent to which sphere size improves photocurrent density J_{sc} is evaluated by carrying out the incident photon to current efficiency (IPCE) of DSSCs. Fig. 4a and b presents

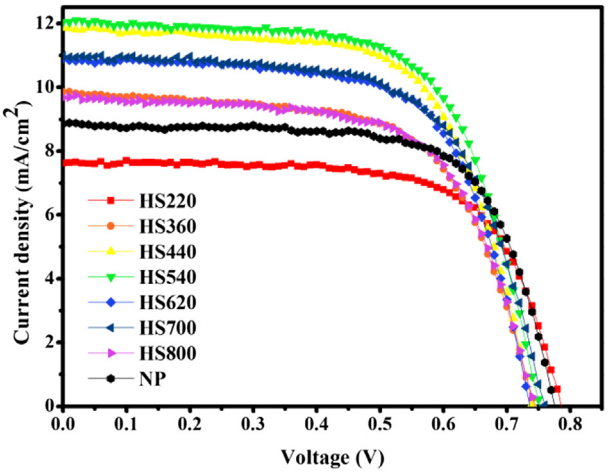

Fig. 3. I–V curves of DSSCs prepared with different sizes of hollow spheres from 220 nm to 800 nm. The DSSC of NP was prepared with rhomboid nanoparticles smashed from hollow spheres.

the IPCE and normalized IPCE of hollow spheres of various sizes, respectively. In Fig. 4a, HS440 and HS550 exhibit the highest IPCE value over the entire spectrum among other DSSCs, which is consistent with the photocurrent measurements for these two cells. Quantum efficiency over the entire visible light region is significantly improved by 450–550 nm hollow spheres, owing to the size compatibility of the hollow sphere and main absorption band of N719 dye molecules. Whereas the small hollow spheres, HS220 and HS360, exhibit extremely poor IPCE values – even inferior to that of NP. Despite having IPCE values as high as HS440 and HS550 cells in the long wavelength region (600–750 nm), HS700 and HS800 have a significantly lower IPCE value in the main absorption region of N719 (400–550 nm). The improved IPCE values in the region of 600–750 nm are generally owing to the light scattering of scatters. In this study, the improvement of IPCE around 600–750 nm region suggests that hollow spheres larger than 440 nm can increase wavelength absorption of N719 dye molecules at 600–750 nm, owing to the scattering effect. One may expect the quantum efficiency of HS700 and HS800 surpasses that of HS450 and HS550 at a long wavelength (over 600 nm) where HS700 and H800 possess intense scattering. However, the quantum efficiency of HS700 and HS800 are still lower than that of HS450 and HS550, which is owing to a low light absorption of dye molecules at this region. In contrast, owing to the less dye adsorption and low scattering ability in visible light region, hollow spheres smaller than 400 nm (i.e. smaller than main absorption spectrum of dye molecules at the visible light region) exhibit an inferior harvest light source.

Based on the above discussion, we conclude that the size of hollow spheres significantly impacts quantum efficiency, subsequently leading to the generation of photocurrent J_{sc}. As is well known, the amount of dye adsorption also affects the IPCE values markedly. According to the literature [36,37], when the photoelectrode thickness is thinner than 13 μm, the IPCE values increase linearly with the thickness. Restated, the IPCE values increase proportionally to the amount of adsorbed dye molecules at 550–650 nm region. The normalized IPCE clearly reveals how size affects the enhancement of a certain wavelength without influence of the dye adsorption (Fig. 4b). As is widely assumed, NP (black solid sphere curve in Fig. 4b) is a standard which does not improve light absorption ability over the entire spectrum by scattering. Above 550 nm, the IPCE value increases with an increasing size of the hollow spheres, indicating that a large sphere enhances the light absorption capacity of long wavelength. Conversely, small hollow spheres such as HS220 and HS360 show the same normalized quantum efficiency spectra over the entire wavelength region as that of NP, implying that hollow spheres smaller than 360 nm do not enhance light absorption capacity.

The extent to which the secondary hierarchical structure affects the light harvested by dye adsorption is more closely examined by using photoelectrodes made by 440 nm solid spheres (SS440), hierarchical hollow spheres (HS440) and another well-known hierarchical structure material, mesoporous spheres (MS440). Fig. 5 shows the SEM images of three TiO_2 anatase spherical particles used as DSSCs photoelectrodes, indicating that all of these spherical particles have a high uniformity and similar sizes. Fig. 6 and Table 3 show the I–V curves and corresponding photovoltaic characteristic parameters, respectively. According to Table 3, HS440 shows a higher J_{sc} of 12 mA cm^{-2}, yet lower V_{oc} of 0.74 V than that of MS440, 10.1 mA cm^{-2} for J_{sc} and 0.79 V for V_{oc}, explaining why both cells perform similarly in terms of efficiency. However, SS440 has an extremely poor efficiency, η of 0.31% owing to an extremely small surface area, resulting in a trace amount of dye adsorption, which is even scarcely detected by UV–vis spectroscopy. According to a previous study, mesoporous spheres uptake a large amount of dye

Table 2
The summary of corresponding photovoltaic characteristic parameters of different sized hollow spheres.

Sample (nm)	Crush	220	360	440	540	620	700	800
V_{oc} (V)	0.783	0.795	0.753	0.75	0.760	0.744	0.770	0.753
J_{sc} (mA cm^{-2})	8.85	7.70	9.95	11.94	12.19	11.00	11.10	9.77
Efficiency (%)	4.86	3.96	4.25	5.58	5.60	5.23	5.14	4.58
Dye adsorption (10^{-9} M cm^{-2} mm^{-1})	11.61	6.38	7.86	8.51	7.95	8.50	9.58	11.32

molecules and scatter visible light efficiently, thus improves the DSSC efficiency significantly [9,20,21]. However, in this study, both hierarchical structure materials, HS440 and MS440, have a similar dye adsorption capacity, suggesting that dye molecules barely diffuse into the central portion of mesoporous spheres, MS440. Moreover, according to our previous study, most resonance scattering happens in the outer shell of a solid sphere [7]. According to the theoretical calculations based on Mie's theory, hollow sphere can still maintain its absorption ability as that of a solid sphere when the ratio between the shell thickness to the sphere diameter is no less than 0.6 for nano-particles with the diameter of 300–900 nm. Consequently, the light harvesting by scattering electromagnetic field occurs near the surface of spheres, even though dye molecules can fully penetrate into the interior of MS440. Finally, a photoelectrode of P25 is prepared in this study for comparison. As expected, HS440 and MS440 display a higher J_{sc}

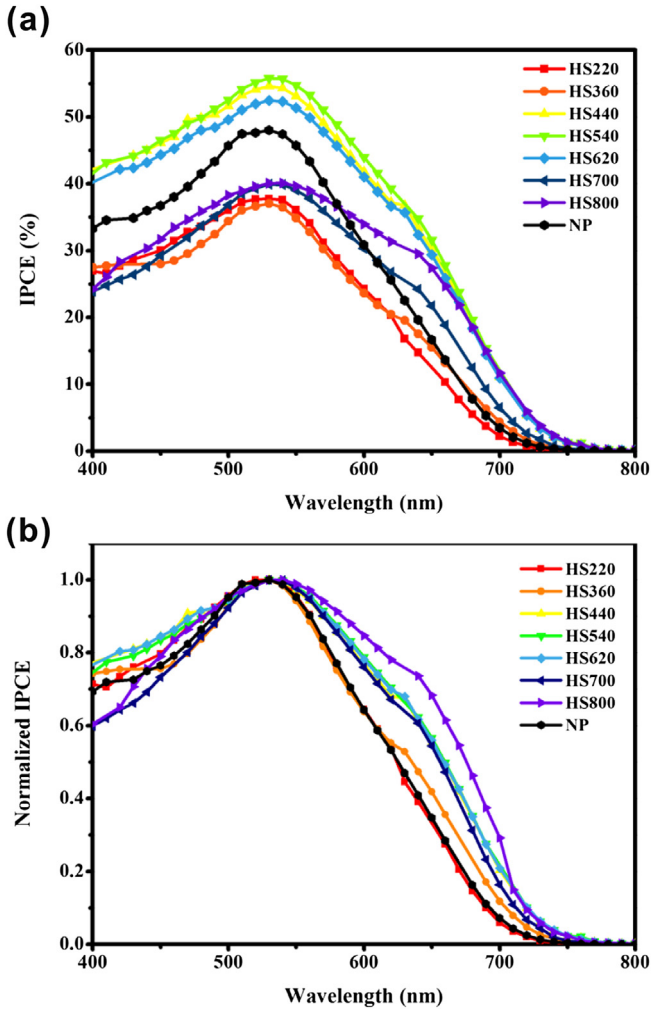

Fig. 4. (a) Incident photon to current conversion efficiency (IPCE) and, (b) normalized IPCE, for the DSSCs prepared with different sized hollow spheres.

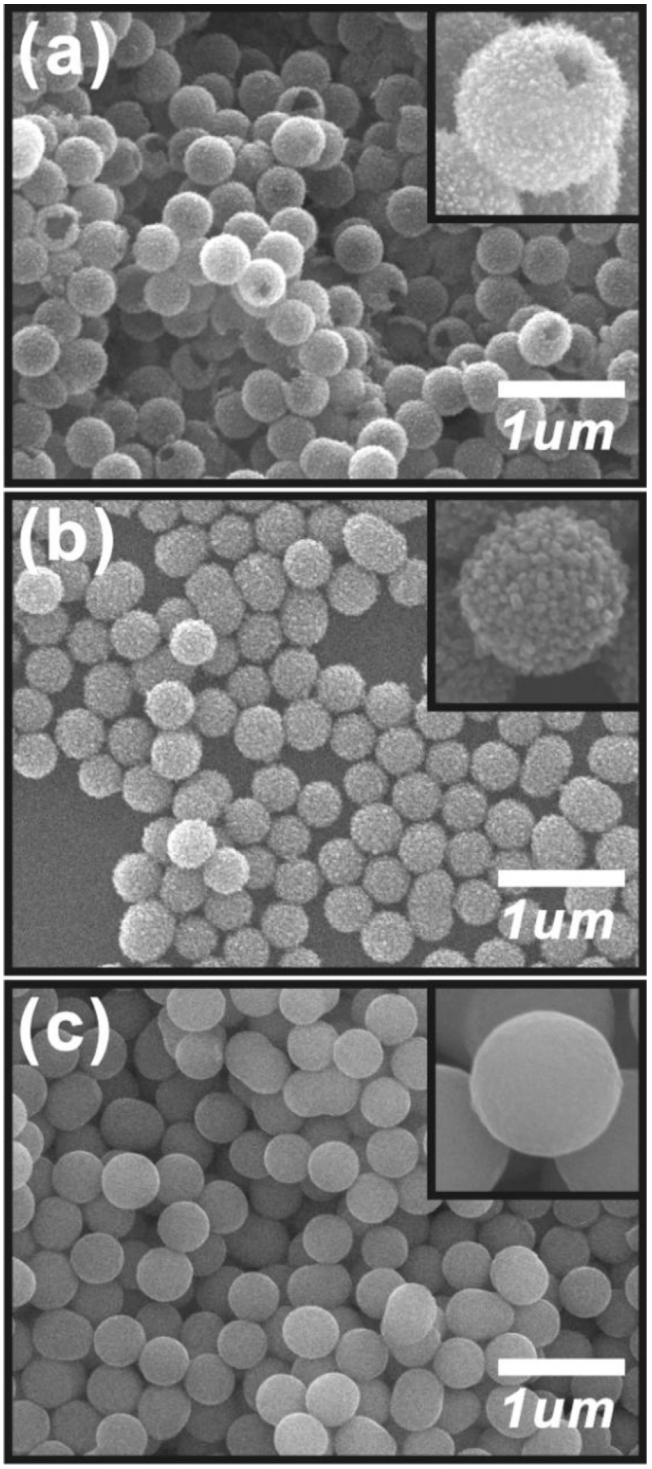

Fig. 5. The SEM images of three different types of spherical anatase TiO_2 utilized as DSSC electrodes. (a) Hierarchical hollow spheres. (b) Hierarchical mesoporous spheres. (c) Solid spheres.

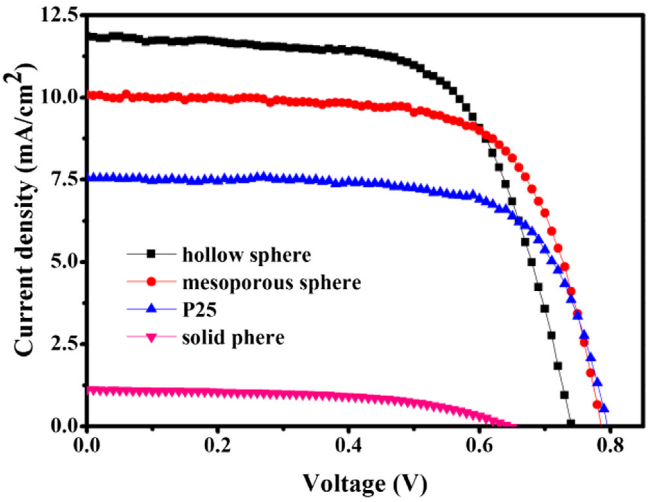

Fig. 6. *I–V* curves of DSSCs prepared with hollow spheres (HS440), mesoporous spheres (MS440), solid spheres (SS440) and P25.

Table 3
The summary of photovoltaic characteristic parameters of hollow spheres (HS440), mesoporous spheres (MS440), solid spheres (SS440) and P25.

Sample (nm)	HS440	MS440	SS440	P25
V_{oc} (V)	0.74	0.79	0.64	0.78
J_{sc} (mA cm^{-2})	12.0	10.1	1.1	7.6
Efficiency (%)	5.70	5.42	0.31	4.23
Dye adsorption (10^{-9} M cm^{-2} mm^{-1})	8.25	7.08	~0	4.17

than P25, owing to a higher surface area and scattering effect, thereby providing a better than P25, which is 4.23%. Based on the above discussion, we believe that hollow spheres are highly promising for use as a photoelectrode in solar cell and other applications with respect to light harvesting such as plasmonic photocatalysis. As is expected, above concepts are applicable to various materials with hierarchical hollow structures and different dye molecules for designing efficient DSSCs and energy devices.

4. Conclusions

In this study, we investigated the size effect of hierarchical hollow spheres synthesized by the self-templating method for DSSC applications. When the size of hierarchical hollow spheres coincides with the main absorption region of dye molecules, 450 nm–550 nm for N719 dyes, the light harvesting can be significantly improved by scattering. When the size of hollow spheres is beyond the main absorption spectrum of dyes, the large-sized hollow spheres over 700 nm can still maintain the quantum efficiency at the longer wavelength. However, hollow spheres with the diameters <360 nm show no enhancement of light harvesting over the entire spectrum. The dye uptake and light harvesting of different spherical hierarchical materials are also examined. According to these results, the hierarchical hollow spheres are superior to mesoporous spheres since the resonant scattering of dye molecules occurs only at the outer region of mesoporous spheres.

Acknowledgments

The authors would like to thank the National Science Council of the Republic of China, Taiwan, for financially supporting this research under Contract No. NSC 101-2113-M-007-012-MY3 and NSC 102-2811-M-007-098. Ted Knoy is appreciated for his editorial assistance.

Appendix A. Supplementary data

Supplementary data related to this article can be found at http://dx.doi.org/10.1016/j.jpowsour.2014.06.015.

References

[1] J.H. Pan, H.Q. Dou, Z.G. Xiong, C. Xu, J.Z. Ma, X.S. Zhao, J. Mater. Chem. 20 (2010) 4512–4528.
[2] F. Sauvage, F. Di Fonzo, A.L. Bassi, C.S. Casari, V. Russo, G. Divitini, C. Ducati, C.E. Bottani, P. Comte, M. Graetzel, Nano Lett. 10 (2010) 2562–2567.
[3] J.Y. Liao, B.X. Lei, D.B. Kuang, C.Y. Su, Energy Environ. Sci. 4 (2011) 4079–4085.
[4] D.P. Wu, F. Zhu, J.M. Li, H. Dong, Q. Li, K. Jiang, D.S. Xu, J. Mater. Chem. 22 (2012) 11665–11671.
[5] Q. Yang, M.Z. Li, J. Liu, W.Z. Shen, C.Q. Ye, X.D. Shi, L. Jiang, Y.L. Song, J. Mater. Chem. A 1 (2013) 541–547.
[6] F. Zhu, D.P. Wu, Q. Li, H. Dong, J.M. Li, K. Jiang, D.S. Xu, RSC Adv. 2 (2012) 11629–11637.
[7] M.C. Tsai, J.Y. Lee, P.C. Chen, Y.W. Chang, Y.C. Chang, M.H. Yang, H.T. Chiu, I.N. Lin, R.K. Lee, C.Y. Lee, Appl. Catal. B Environ. 147 (2014) 499–507.
[8] S. Dadgostar, F. Tajabadi, N. Taghavinia, ACS Appl. Mater. Interfaces 4 (2012) 2964–2968.
[9] Y.J. Kim, M.H. Lee, H.J. Kim, G. Lim, Y.S. Choi, N.G. Park, K. Kim, W.I. Lee, Adv. Mater. 21 (2009) 3668–3673.
[10] P.C. Chen, M.C. Tsai, M.H. Yang, T.T. Chen, H.C. Chen, I.C. Chang, Y.C. Chang, Y.L. Chen, I.N. Lin, H.T. Chiu, C.Y. Lee, Appl. Catal. B Environ. 142 (2013) 752–760.
[11] M.H. Yang, M.C. Tsai, Y.W. Chang, Y.C. Chang, H.T. Chiu, C.Y. Lee, ChemCatChem 5 (2013) 1871–1876.
[12] P.C. Chen, M.C. Tsai, H.C. Chen, I.N. Lin, H.S. Sheu, Y.S. Lin, J.G. Duh, H.T. Chiu, C.Y. Lee, J. Mater. Chem. 22 (2012) 5349–5355.
[13] Y.S. Lin, M.C. Tsai, J.G. Duh, J. Power Sources 214 (2012) 314–318.
[14] Y.S. Lin, J.G. Duh, M.C. Tsai, C.Y. Lee, Electrochim. Acta 83 (2012) 47–52.
[15] G.L. Shang, J.H. Wu, M.L. Huang, Z. Lan, J.M. Lin, Q. Liu, M. Zheng, J.H. Huo, L. Liu, J. Mater. Chem. A 1 (2013) 9869–9874.
[16] M.D. Ye, H.Y. Liu, C.J. Lin, Z.Q. Lin, Small 9 (2013) 312–321.
[17] Z.Y. Yin, Z. Wang, Y.P. Du, X.Y. Qi, Y.Z. Huang, C. Xue, H. Zhang, Adv. Mater. 24 (2012) 5374–5378.
[18] F. Chu, W. Li, C.S. Shi, E.Z. Liu, C.N. He, J.J. Li, N.Q. Zhao, ACS Appl. Mater. Interfaces 5 (2013) 7170–7175.
[19] J.H. Park, S.Y. Jung, R. Kim, N.-G. Park, J. Kim, S.-S. Lee, J. Power Sources 194 (2009) 574–578.
[20] J.G. Yu, J.J. Fan, B. Cheng, J. Power Sources 196 (2011) 7891–7898.
[21] H. Xu, X.Q. Chen, S.X. Ouyang, T. Kako, J.H. Ye, J. Phys. Chem. C 116 (2012) 3833–3839.
[22] Q.F. Zhang, T.R. Chou, B. Russo, S.A. Jenekhe, G.Z. Cao, Angew. Chem. Int. Ed. 47 (2008) 2402–2406.
[23] Q.F. Zhang, T.P. Chou, B. Russo, S.A. Jenekhe, G. Cao, Adv. Funct. Mater. 18 (2008) 1654–1660.
[24] Y. Kondo, H. Yoshikawa, K. Awaga, M. Murayama, T. Mori, K. Sunada, S. Bandow, S. Iijima, Langmuir 24 (2008) 547–550.
[25] C.X. He, B.X. Lei, Y.F. Wang, C.Y. Su, Y.P. Fang, D.B. Kuang, Chem.-Eur. J. 16 (2010) 8757–8761.
[26] J.G. Yu, J.J. Fan, L. Zhao, Electrochim. Acta 55 (2010) 597–602.
[27] X.H. Song, M.Q. Wang, T.Y. Xing, J.P. Deng, J.J. Ding, Z. Yang, X.Y. Zhang, J. Power Sources 253 (2014) 17–26.
[28] D.H. Chen, F.Z. Huang, Y.B. Cheng, R.A. Caruso, Adv. Mater. 21 (2009) 2206.
[29] C. F. Bohren and D. R. Huffman, Absorption and Scattering of Light by Small Particles, Wiley, New York, 1983..
[30] I.G. Yu, Y.J. Kim, H.J. Kim, C. Lee, W.I. Lee, J. Mater. Chem. 21 (2011) 532–538.
[31] Y.C. Park, Y.J. Chang, B.G. Kum, E.H. Kong, J.Y. Son, Y.S. Kwon, T. Park, H.M. Jang, J. Mater. Chem. 21 (2011) 9582–9586.
[32] M.C. Tsai, T.L. Tsai, C.T. Lin, R.J. Chung, H.S. Sheu, H.T. Chiu, C.Y. Lee, J. Phys. Chem. C 112 (2008) 2697–2702.
[33] M.C. Tsai, T.L. Tsai, C.T. Lin, R.J. Chung, H.S. Sheu, H.T. Chiu, C.Y. Lee, Anal. Chem. 81 (2009) 7590–7596.
[34] J.G. Yu, J.C. Yu, M.K.P. Leung, W.K. Ho, B. Cheng, X.J. Zhao, J.C. Zhao, J. Catal. 217 (2003) 69–78.
[35] J.G. Yu, S.W. Liu, H.G. Yu, J. Catal. 249 (2007) 59–66.
[36] M.G. Kang, K.S. Ryu, S.H. Chang, N.G. Park, J.S. Hong, K.J. Kim, Bull. Korean Chem. Soc. 25 (2004) 742–744.
[37] L.I. Halaoui, N.M. Abrams, T.E. Mallouk, J. Phys. Chem. B 109 (2005) 6334–6342.